

BaTiO₃ properties and powder characteristics for ceramic capacitors

Dang-Hyok Yoon and Burtrand I. Lee*

School of Materials Science and Engineering, Olin Hall, 340971, Clemson University, Clemson, SC 29634-0971, USA

Barium titanate (BaTiO₃) is one of the most widely used ceramic raw materials in the electro-ceramic industry, especially in multi-layer ceramic capacitors (MLCCs). In this paper recent information on basic dielectric properties, the effect of particle size on phase transition, and powder characteristics resulting from various synthetic methods of producing BaTiO₃, including the hydrothermal method are reviewed.

Key words: BaTiO₃, Dielectric property, MLCC, Hydrothermal.

Introduction

Since the discovery of ferroelectricity in barium titanate (BaTiO₃) in the 1940s [1], much research has been carried out on this ceramic material. Nowadays multilayer ceramic capacitors (MLCCs) based on BaTiO₃ are one of the most important electronic components in surface mounted electronic circuits. Common electronic appliances contain many MLCCs, *e.g.*, a typical watch contains 2-4, a video camera or cell phone 250, a laptop computer 400 and an automobile over 1000.

MLCCs, as shown in Figure 1, have alternating layers of dielectric materials and internal metal electrodes. Until 1995 most MLCCs were fabricated using expensive inner electrode materials such as the precious metals

palladium (Pd) or palladium-silver alloys (Pd/Ag) [2, 3]. The tremendous increase in the price of Pd during the past few years has accelerated the use of base metal electrodes (BME) such as nickel (Ni) and copper (Cu) in MLCCs [2, 3]. Changing to Ni electrodes may reduce the cost 50-80% compared to the cost of the precious metal electrodes [4]. Increasingly more than 60% of MLCCs with a great volumetric efficiency with 2-3 μm dielectric layer thickness of several hundred layers, are manufactured with Ni base metal electrodes [3, 4].

Two features may be discussed that led to the present high degree of interest in MLCCs. One is the discovery of the ferroelectric properties of barium titanate and its high relative dielectric constant. The other is the technical breakthrough for making multilayer ceramic units in a small volume, thus satisfying the need for an economical manufacture of systems, and the requirements for printed circuit boards and for hybrid circuits on ceramic substrates. The MLCC production process needs a combination of many different fields of knowledge, including powder processing, slip behavior, thick-film manufacturing, interaction between metal and dielectrics, sintering behavior in a reducing atmosphere, etc. Most of all, understanding the dielectric properties of BaTiO₃ and the powder characteristics are prerequisites for further understanding the MLCCs process. As the demand for volumetric efficiency of electronic devices increase, MLCCs need thinner dielectric layers. This will require finer BaTiO₃ particles with stringent powder characteristics.

Among the various methods for producing submicrometer BaTiO₃ powder, the hydrothermal technique is well known. Although this technique produces fine particles of BaTiO₃ with acceptable particle morphology and composition, the product needs much improvement to meet the current and future demand.

Therefore, our review focuses on the recent development of these two aspects of BaTiO₃ powder, *i.e.*, basic

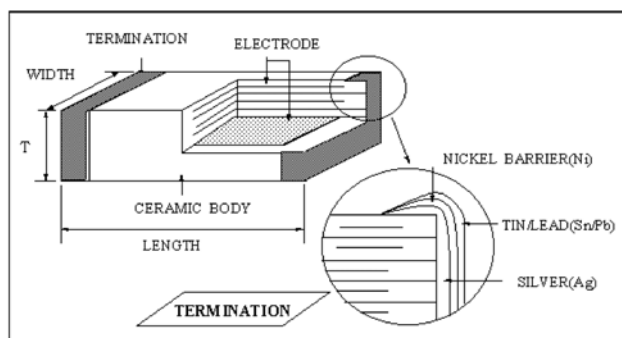


Fig. 1. A cutaway view and photograph of multilayer ceramic chip capacitors (MLCCs).

*Corresponding author:

Tel : +1-864-656-5348

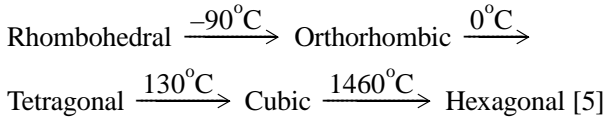
Fax: +1-864-656-1453

E-mail: dyoon@clemson.edu; burt.lee@ces.clemson.edu

dielectric properties of BaTiO₃ and the characteristics of various synthetic BaTiO₃ powders.

Basic Dielectric Properties of BaTiO₃

BaTiO₃ undergoes crystalline phase transitions with temperature:



Because of the practical temperature ranges, the tetragonal phase and the tetragonal to cubic phase transition region are important. The tetragonal to cubic transition temperature is usually called a Curie point. The Curie point is generally located at 120–130°C, although the Curie point is known to decrease to 75°C accompanied by a decrease in the particle size of BaTiO₃ from 1.0 μm to 0.12 μm [6].

In the temperature range for the cubic phase, *i.e.*,

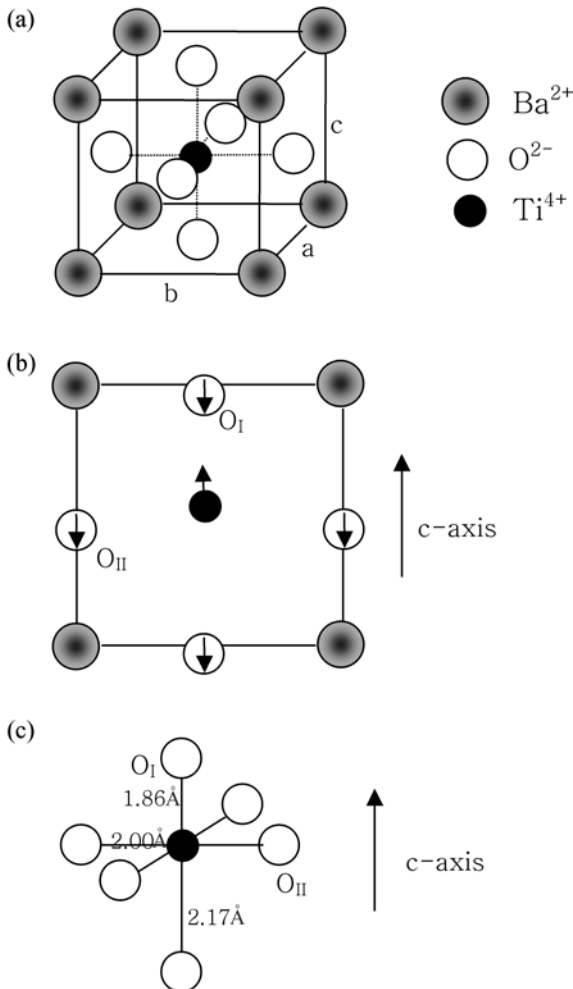


Fig. 2. (a) Perovskite structure of BaTiO₃ above Curie point, (b) a-axis projection of tetragonal BaTiO₃ with atomic displacements, and (c) Unit is not printed. For all values such as 1.86, 2.00 and 2.17, we need the Å unit.

above the Curie point, the ideal perovskite structure of a cubic and symmetrical unit cell is stable. Between 0° and 130°C, BaTiO₃ shows a distorted perovskite structure in which the Ti⁴⁺ and O²⁻ ions are displaced in the opposite direction from their original positions, whereas the barium ion does not change its position. This results in a large change of the Ti-O bond length compared to a small change in the Ba-O bond during the cubic to tetragonal phase changes [7]. A perovskite lattice structure, the displacement of the Ti⁴⁺ and O²⁻ ions and the slight distortion of oxygen octahedra during the cubic to tetragonal phase transition are shown in Fig. 2 [8]. These ionic displacements also result in a change in lattice dimensions, and a negative linear thermal expansion coefficient along the c-axis, while a thermal expansion coefficient is usually positive due to a-, b-axes expansion (Fig. 3) [9]. As shown in Figure 3, the crystal structure of BaTiO₃ becomes less and less tetragonal as the temperature increases toward the tetragonal to cubic transition temperature.

Cubic BaTiO₃ shows paraelectric properties, while tetragonal BaTiO₃ shows ferroelectric properties which are more interesting properties of BaTiO₃ for dielectric applications. The relative dielectric constant variations along a-, b- and c-axes of the single crystalline BaTiO₃ are given in Fig. 4 [10]. An explanation of why the dielectric constant along the c-axis is less than that along the a-axis is that oxygen ions in the c-axis, which is also cell polar axis, make strong ionic attractions with the center Ti⁴⁺ ion. This gives an interaction force between the Ti⁴⁺ and O²⁻ ions which makes vibration difficult because of a “pinning” effect under an external AC source. On the other hand, oxygen ions in the a- and b-axes are relatively free to vibrate perpendicularly to this c-axis, consequently, the dielectric constants along a- and b-axes are higher. In the vicinity of the Curie point, the stability of the lattice decreases and the

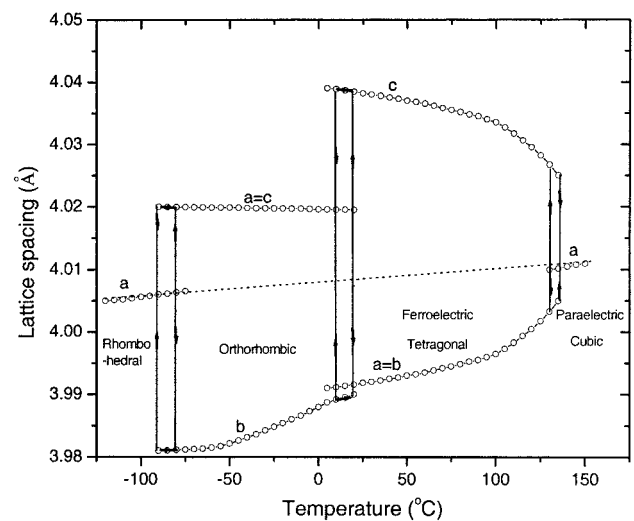


Fig. 3. Lattice parameters of single crystal BaTiO₃ as a function of temperature. [9]

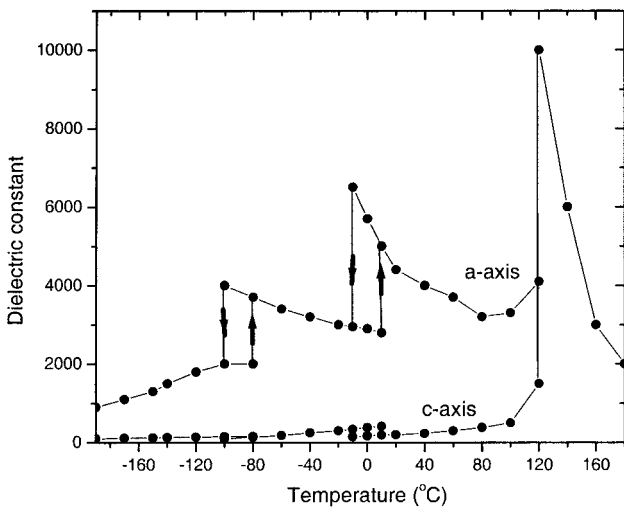


Fig. 4. Relative dielectric constant ϵ_a and ϵ_c for single crystal BaTiO₃ as a function of temperature. [10]

amplitude of the vibration becomes higher. This induces a high dielectric constant at the Curie point. Based on these dielectric properties of a single crystal, we can infer the dielectric behavior of the polycrystalline sample or powder which is the starting material for MLCC fabrication. The dielectric constant of polycrystalline, non-polarized BaTiO₃, is an average of both curves in Fig. 4 due to the random orientation of the individual crystals.

Although the basic dielectric properties are well known, it is worthwhile to note that the physical parameters related to the phase transition are affected by chemical purity, surface defects, particle size [6, 12] and sintering conditions as Jaffe *et al.* explained [11]. Among these factors, understanding the relationship between particle size and tetragonality is especially important. This is

because a recent preference for producing thinner dielectric layers and lowering sintering temperatures is dependent on fine particle size. Generally the belief is that there is a decrease in tetragonal distortion with decreasing particle size below approximately 1 μm . Uchino *et al.* [6] showed that the transformation from tetragonal to cubic symmetry occurred at a critical particle size of 0.12 μm at 75°C. Begg *et al.* [13], however, indicated that a hydrothermal BaTiO₃ powder with a particle size larger than 0.27 μm was completely tetragonal and with a particle size less than 0.19 μm was a fully cubic phase as shown by X-ray diffraction (XRD) and electron microscopy. More details on the critical particle size vs. the phase transition are presented in Table 1. All the reports show some difference in the critical particle size. This critical size difference may come from the different residual elastic strain energy, chemical impurity level and crystalline defects.

Two models have been proposed to describe the room temperature stabilization of the cubic structure in fine-grained BaTiO₃. One is the phenomenological surface layer model [14], and the other is the pure phase model [6, 22].

The phenomenological surface layer model is based on the structural transition between the outer cubic surface layer of fixed thickness and the tetragonal core, with a gradient of tetragonality existing between the two regions. As the particle size decreases, the relative ratio of cubic to tetragonal region is increased and eventually only a stable cubic region remains at a critical particle size. As an example, Takeuchi *et al.* [17], using a BaTiO₃ powder formed by a solid-state reaction, estimated the thickness of the surface cubic layer as 5.1 nm, independent of the particle size by XRD measurement.

Table 1. Critical particle sizes for the cubic to tetragonal phase transition

Researcher	Results	Preparation method	Measurement method
Arlt <i>et al.</i> [15]	$\leq 0.5 \mu\text{m}$ pseudocubic	oxalate	XRD, ϵ_r measurement
Uchino <i>et al.</i> [6]	$\leq 0.12 \mu\text{m}$ cubic $> 0.12 \mu\text{m}$ tetragonal	hydrothermal, solid-state coprecipitation	XRD, BET
Hennings and Schreinemacher [16]	0.2–0.4 μm cubic $\leq 0.15 \mu\text{m}$ cubic $\geq 0.20 \mu\text{m}$ tetragonal	hydrothermal solid-state solid-state	XRD
Begg <i>et al.</i> [13]	$\leq 0.19 \mu\text{m}$ cubic $\geq 0.27 \mu\text{m}$ tetragonal	hydrothermal	XRD, SEM, HRTEM
Takeuchi <i>et al.</i> [17]	0.32–1.22 μm coexistence	solid-state	XRD
Lobo <i>et al.</i> [18]	$\geq 0.2 \mu\text{m}$ tetragonal	sol-gel	XRD, ϵ_r measurement
Li and Shih. [19]	$\leq 0.056 \mu\text{m}$ cubic $\geq 0.071 \mu\text{m}$ tetragonal	alkoxide-hydroxide	XRD
Jiang <i>et al.</i> [20]	0.105–0.130 μm Cubic to tetragonal change	sol-gel	Raman spectroscopy XRD
Lu <i>et al.</i> [21]	0.01–3.5 μm cubic 0.08 μm Cubic with some tetragonal	stearic-acid gel hydrothermal	XRD, DSC Raman spectroscopy

The pure phase model does not require the coexistence of the cubic and tetragonal structures. There are two mechanisms to explain this model; strains imposed by the presence of lattice hydroxyl ions [22] and the role of the surface [6]. Regarding the hydroxyl ion effects, Vivekanandan and Kutty [22] explained the source of lattice strain from point defects caused by the presence of hydroxyl ions and the corresponding cation vacancies. According to Vivekanandan and Kutty, the residual hydroxyl ions in the oxygen sub-lattice, the structure is retained during hydrothermal BaTiO₃ synthetic process, are compensated by cation vacancies, and result in strain leading to the metastable presence of the cubic phase at room temperature. Although one can remove hydroxyl ions completely by annealing in air at 900°C for 15 hours, BaTiO₃ still remains as a cubic phase by the retained strain of compensating cation vacancies. Only with annealing above 1000°C, is the tetragonal phase acquired.

However, retention of the supposed charge-compensating cation vacancies is difficult to visualize once the hydroxyl ions have been removed from the lattice. Therefore, Begg *et al.* [13] used Vivekanandan and Kutty's model to explain the deficiency with regard to the role of hydroxyl ions/cation vacancies in the stabilization of the cubic structure. Begg *et al.* [13] observed that the tetragonal hydrothermal BaTiO₃ powder contained more hydroxyl ions than the cubic phase BaTiO₃.

The surface effect model is based on the surface tension associated with the very fine powder stabilizing the cubic phase at room temperature. Uchino *et al.* [6] observed that a decrease of room temperature tetragonality and the Curie point are a function of the reduction in particle size. According to Uchino *et al.* [6], this surface tension is sufficiently high to decrease the tetragonality and the Curie point associated with small particle size barium titanate.

In summary, due to the importance of fine sized tetragonal BaTiO₃, many researchers have been interested in the cubic to tetragonal phase transition of this powder. However, all the research reports show different results on the critical particle size produced by different synthetic methods and different measurement methods. This critical size difference may come from the different residual elastic strain energy, chemical impurity levels and crystalline defects. More research will be required.

Properties of BaTiO₃ Powder

By considering the MLCC production processes, the desired powder properties can be clearly defined. During the MLCC production processes, a mixture of ceramic powders and binder solution are formed into green ceramic sheets by tape casting. Subsequent steps include screen printing of the internal electrode on the green sheet, stacking to obtain the desired number of layers,

laminating, cutting, binder burn-out, sintering, etc.

Currently, production of MLCCs of two to three micrometers thick green ceramic sheets containing several hundred layers yields the highest volumetric efficiency. If one of these layers contains small air pockets or pores which originate from poor powder dispersion, failure of the final products results. In practice, each sintered layer needs more than 5 grains to give long-term stability to the final products [4]. Therefore, MLCC manufacturers desire BaTiO₃ powders with spherical, chemically homogeneous, unagglomerated, submicrometer and nearly monodispersed particles in order to get the favorable green microstructure.

Processes for the synthesis of fine BaTiO₃ powder utilize a wide variety of methods including a solid-state reaction [23], coprecipitation (*e.g.*, citrates [24], oxalates [25]), hydrothermal synthesis [26], alkoxide hydrolysis [27], and metal-organic processing [28]. In addition, other processes studied include the solvothermal synthesis [29] which corresponds to the hydrothermal method except for the use of a solvent other than water, and the low-temperature aqueous synthesis (LTAS) [30] method at atmospheric pressure. After considering properties and cost of the various kinds of methods, the solid-state reaction, oxalate and calcined hydrothermal BaTiO₃ powders are currently the most commonly used powder in MLCC industry.

Easy uniform dispersion, lower firing temperature with a minimum amount of sintering aids, higher dielectric constant, lower dissipation factor, higher sintering density and easier control of properties with less variation are the most desired properties of BaTiO₃ in MLCC industries.

The solid-state reaction method is the traditional method for preparing BaTiO₃ powders by mixing the starting materials, usually titanium oxide and barium carbonate, and calcining them at an elevated temperature around 1100°C. However, the solid-state reaction method tends to result in a significant amount of agglomeration, poor chemical homogeneity and undesired secondary phase such as BaTi₂O₅.

The oxalate method, based on the coprecipitation of a complex of Ba and Ti ions as oxalates, requires controlled solution pH, temperature and concentration of the solutes. Calcination of the product at 600-700°C produces the BaTiO₃ final product. This procedure allows tight control over stoichiometry, leads to a high-purity product, and makes it easy to dope the products by coprecipitation. Separation, washing and drying of the precipitate precede calcination. Due to the exothermic calcination process, this produces soft agglomeration.

The hydrothermal method, which belongs to the category of liquid phase reactions, characteristically produces extremely fine particles with high crystallinity, high purity, fewer dislocations and a narrow size distribution containing spherical morphology [22]. This technique involves heating an aqueous suspension of

insoluble salts in an autoclave at a moderate temperature and pressure so that the crystallization of a desired phase will take place. The advantages of hydrothermal crystallization are the reduced energy costs due to the moderate temperatures sufficient for the reaction, less pollution, simplicity in the process equipment, and the enhanced rate of the precipitation reaction [22]. The possible variables affecting the particle size and shape are the concentration of starting materials, hydrothermal temperature and reaction time. The particle size of hydrothermally synthesized BaTiO₃ is usually less than 200 nm. This size is smaller than that which the MLCC industry currently needs. Generally for MLCCs, the recommendation is to use 300-500 nm particle size for easy dispersion, a thinner dielectric layer and a higher relative dielectric constant of the sintered body. Therefore, BaTiO₃ manufacturers increase the hydrothermal particle size by heat treatment at around 1000°C. Due to this heat treatment and the following milling process, the resulting powder to some degree contains the same drawbacks as the powder produced by the solid-state reaction, *i.e.*, hard agglomerates and irregular particle shape. However, technical breakthroughs have overcome these drawbacks by making it possible to grow a particle size up to 400 nm with only hydrothermal treatment [31].

Figure 5 shows Scanning Electron Microscope (SEM) micrographs of BaTiO₃ produced by different synthetic methods. As one can see, the hydrothermal powder with milling after heat treatment (b) has almost the same irregular morphology as that of traditional solid-state reaction powder (a). On the other hand, BaTiO₃ powder grown only using a hydrothermal process (c) has a spherical shape and uniform particle size distribution which is the most favorable particle shape for MLCC industrial use.

However, the chemical properties of BaTiO₃ powder should be considered at this point. Due to their unique synthetic history and handling methods, differently synthesized BaTiO₃ powders show their own characteristics. For example, Jiang *et al.* [20] showed a clear difference in phase transition behavior and defect structure between sol-gel derived powders and stearic acid-gel derived BaTiO₃ ultra-fine particles. According to them, sol-gel derived powders showed low defect density and a strong particle size dependence on the tetragonal to cubic phase transition, while stearic acid-gel derived powder showed many more internal defects and an abnormal phase transition at 200 K, which was quite different from the normal barium titanate characteristics.

Except for this difference in internal defects, reports note that incorporated ionic or surface adsorbed species during synthesis and/or storage could change the powder characteristics [32-36]. The ionic species which can most likely affect the powder characteristics are the hydroxyl (OH⁻), the proton (H⁺) [37] and the carbonate

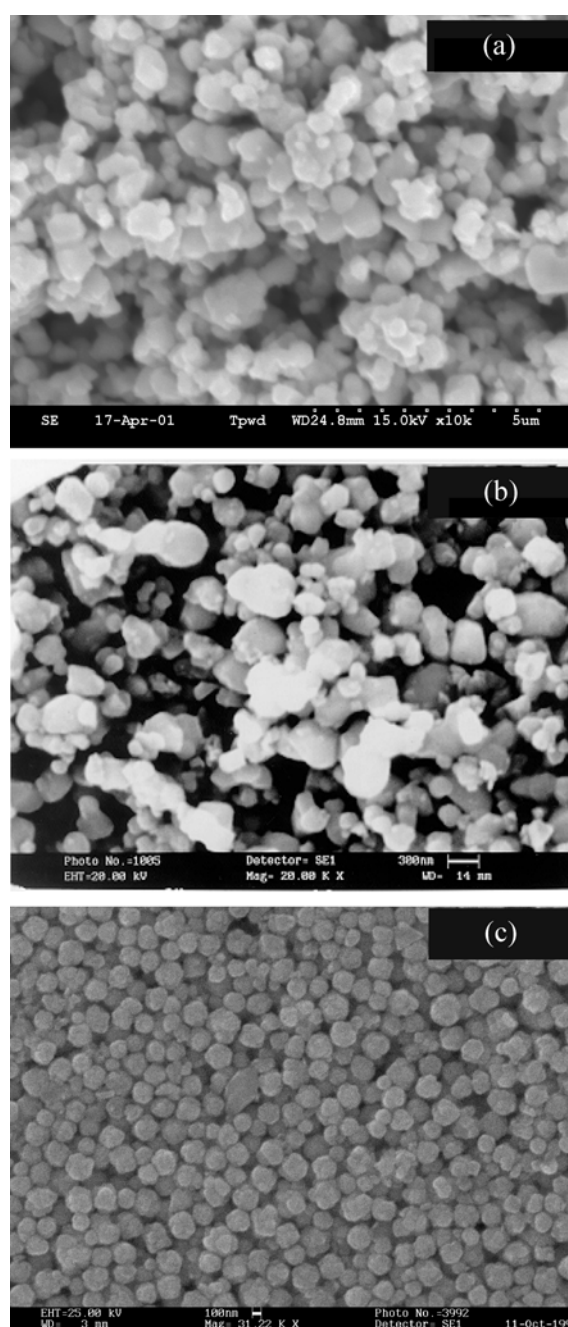


Fig. 5. SEM micrographs of 3 kinds of commercial BaTiO₃ powders. (a) solid-state reaction powder, (b) hydrothermal & heat-treated powder and (c) hydrothermal powder.

(CO₃²⁻) [38]. Lee [38] explained the possibility of a carbonate effect on lot-to-lot variation in commercial BaTiO₃ powders, as well as a carbonate effect on Ba²⁺ dissolution in an aqueous system.

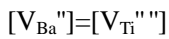
Hennings *et al.* [37] pointed out the role of protons and hydroxyl ions which were incorporated into the lattice of the BaTiO₃ powder during the hydrothermal synthesis. They also observed that MLCCs made with hydrothermal powder showed a strange expansion at the final stage of sintering which they called “bloating”. This was absent in the powder derived from a solid-

state reaction. Due to the process characteristics, protons and hydroxyl ions can be easily incorporated into the lattice in the hydrothermal process. According to Hennings *et al.* [37], hydrothermal powder can incorporate large amounts of protons (≈ 0.4 mol/mol BaTiO_3) in the oxygen lattice sites by generating metal ion vacancies for the charge compensation. As a result, a considerable enlargement of the unit cell volume, which gives a particle density lower than the ideal density, and a suppression of the tetragonal distortion of the perovskite unit cell were observed [16]. When the powder is annealed in the 500-800°C temperature range, metal ions and oxygen vacancies combine into small nanometer-sized intragranular pores. No intragranular pores form when annealing occurs at less than 400°C or more than 800°C, according to the High Resolution Transmission Electron Microscope (HRTEM) results. This means that calcination at 500-800°C expels OH^- or water leaving 4-5 vol.% of pores behind. Even though there are many protons, they remain as point defects at lower temperatures, *e.g.*, 400°C. These defects could not be seen through HRTEM. In powders annealed at temperatures higher than 800°C, the combined intragranular pores are released during the annealing. Therefore, detection of intragranular pores did not occur in such annealed powder.

Hennings *et al.* [37] explained these phenomena with the following defect equation. Barium and titanium vacancies simultaneously compensated for the lattice-incorporated protons and correspondingly, the OH groups at oxygen sites:



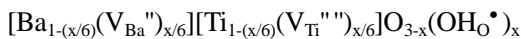
In the case of the monophasic situation, the number of vacancies on the A- and B- sites must be equal to each other:



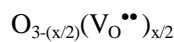
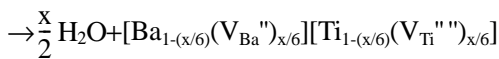
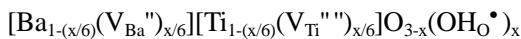
Then, by the charge balance condition:



The resultant defect chemical formula for BaTiO_3 that contains x mol $[\text{OH}_0^\bullet]$ per mol of perovskite, which are compensated by vacancies on the A- and B- sites, is:

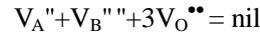


During the annealing at 500~800°C, oxygen vacancies are formed by the following equation:

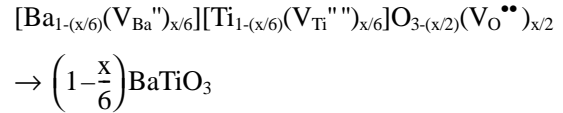


Because of the unstable nature of a structure containing a large number of barium, titanium and oxygen

vacancies, annihilation of these defects occurs during high temperature annealing at temperature greater than 800°C:



If most of the point defects have disappeared at a higher temperature, BaTiO_3 powder shows a volumetric reduction and higher density, which is the almost same as the ideal density described by the following equation:



In summary, hydrothermally synthesized BaTiO_3 can show an adverse effect such as bloating in the final stage of the sintering process due to its inherently incorporated hydroxyl ions and protons during the synthetic process, despite the ideal uniform size and spherical particle shape.

Outlook

In recent years, the worldwide electronic industry has continued to develop high density and high frequency systems and devices. To keep up with this trend, ceramic electronic components need to be smaller, faster, lighter and of lower cost. Significant advances have been achieved in reduction of dielectric thickness to increase the volumetric efficiency of MLCCs. The MLCCs having the highest volumetric efficiency are currently less than 3 μm thick and are comprised of 5 hundred of dielectric layers [3, 4]. These conditions result in 20 μF capacitance. However, critical processes in the manufacture of MLCCs including materials formulation, powder processing, tape casting and sintering must be carefully controlled to ensure reproducibility and reliability. In addition, better understanding of the physical and chemical properties of BaTiO_3 powder is essential for advanced MLCCs.

Acknowledgements

This material is based upon work supported by the National Science Foundation under Grant No. DMR-9731769. Any opinions, findings and conclusions or recommendations expressed in this material are those of the authors and do not necessarily reflect the views of the National Science Foundation.

References

1. W. Kanzig, *Ferroelectricity*. 74 (1987) 285-291.
2. Y. Sakabe, in *Proceedings of the 9th US-Japan Seminar on Dielectric and Piezoelectric Ceramics*, November 1999, (Japan, 1999) p. 1.
3. D. F. K. Hennings, *J. Eur. Ceram. Soc.* 21 (2001) 1637-1642.

4. Y. Sakabe, in "Multilayer Electronic Ceramic Devices" (The American Ceramic Society, Ohio, U.S.A., 1999) p. 3.
5. J. G. Dickson, Lewis Katz and Rolland Ward, J. Am. Chem. Soc. 83 (1961) 3026-3029.
6. K. Uchino, E. Sadanaga and T. Hirose, J. Am. Ceram. Soc. 72[8] (1989) 1555-1558.
7. W. Cochran, Adv. Phys. 9 (1960) 387-406.
8. V. Anuradha, "NMR Study of Quardrupolar Nuclei in Some Simple Cubic and Perovskite Compounds."; Masters Thesis. University of Warwick. U.K., 1990.
9. R. Clarke, J. Appl. Cryst. 9 (1976) 335-338.
10. W. J. Merz, Phys. Rev. 76[8] (1949) 1221-1225.
11. B. Jaffe, W. R. Cooke and H. Jaffe, in "Piezoelectric Ceramics" (Academic press, 1971) p. 53.
12. K. Kinoshita and A. Yamaji, J. Appl. Phys. 47[1] (1976) 371-373.
13. B. D. Begg, E. R. Vance and J. Nowotny, J. Am. Ceram. Soc. 77[12] (1994) 3186-3192.
14. J. C. Niepce, in "Surfaces and Interfaces of Ceramic Materials" (Kluwer Academic Publishers, Dordrecht, Netherlands, 1989) p. 512.
15. G. Arlt, D. Hennings and G. de With, J. Appl. Phys. 58[4] 15 (1985) 1619-1625.
16. D. Hennings and S. Schreinemacher, J. Eur. Ceram. Soc. 9 (1992) 41-46.
17. T. Takeuchi, K. Ado, T. Asai, H. Kageyama, Y. Saito, C. Masquelier and O. Nakamura, J. Am. Ceram. Soc. 77[6] (1994) 1665-1668.
18. R. Lobo, D. Mohallem and R. Moreira, J. Am. Ceram. Soc. 78[5] (1995) 1343-1346.
19. X. Li and W. Shih, J. Am. Ceram. Soc. 80[11] (1997) 2844-2952.
20. B. Jiang, J.L. Peng, L.A. Bursill, T.L. Ren, P.L. Zhang and W.L. Zhong, Physica B. 291 (2000) 203-212.
21. S.W. Lu, B.I. Lee, Z.L. Wang and W.D. Samuels, J. Cryst. Growth. 219 (2000) 269-276.
22. R. Vivekanandan and T.R.N. Kutty, Powder Technology. 57 (1989) 181-192.
23. L.K. Templeton and J.A. Pask, J. Am. Ceram. Soc. 42 (1959) 212-216.
24. B.J. Mulder, J. Am. Ceram. Soc. Bull. 49 (1970) 990-993.
25. M. Stockenhuber, H. Mayer, and J.A. Lercher, J. Am. Ceram. Soc. 76[5] (1993) 1185-1190.
26. H. Kumazawa, S. Annen and E. Sada, J. Mat. Sci. 30 (1995) 4740-4744.
27. P.P. Phule, S. Raghavan and S. H. Risbud, J. Am. Ceram. Soc. 70[5] (1987) C-108-C-109.
28. A.S. Shaikh and G.M. Vest, J. Am. Ceram. Soc. 69 (1986) 682-688.
29. D. Chen and X. Jiao, J. Am. Ceram. Soc. 83[10] (2000) 2637-2639.
30. M. Viviani, J. Lemaitre, M.T. Buscaglia and P. Nanni, J. Eur. Ceram. Soc. 20 (2000) 315-320.
31. S.V. Venigalla, D.V. Miller, J.A. Kerchner, D.J. Clancy, K.A. Thrush and S.A. Costantino, in Proceedings of the 9th US-Japan Seminar on Dielectric and Piezoelectric Ceramics, November 1999, (Japan, 1999) p. 319.
32. C. Herard, A. Faivre and J. Lemaitre, J. Eur. Ceram. Soc. 15 (1995) 135-144.
33. C. Herard, A. Faivre and J. Lemaitre, J. Eur. Ceram. Soc. 15 (1995) 145-153.
34. D. Lee and R.A. Condrate Sr., Mater. Res. Soc. Symp. Proc. 458 (1997) 385-388.
35. B.I. Lee, J. Electroceram. 3[1] (1999) 51-61.
36. S.W. Lu, B.I. Lee and L.A. Mann, Mater. Lett. 43 (2000) 102-105.
37. D.F.K. Hennings, C. Metzmacher and B.S. Schreinemacher, J. Am. Ceram. Soc. 84[1] (2001) 179-182.
38. B.I. Lee, J. Electroceram. 3[1] (1999) 53-63.